A Low-Profile Dual-Band RFID Antenna Combined With Silence Element

Yongqiang Chen, Huiping Guo, Xinmi Yang, Xueguan Liu
School of Electronics and Information Engineering, Soochow University, SuZhou, China 215006

***Abstract*—A low-profile dual-band three-dimensional antenna covering bands of 915 MHz and 2.45 GHz is proposed for radio frequency identification (RFID) applications. The eighth-wavelength antenna utilizes the planar triangular patches and a disk to reduce the profile. Planar tuning patches are adopted to replace the conventional tuning poles for improving the impedance matching. Silence element, defined as a radiator with little influence on others, is composed of quarter-wavelength patch working at higher band in this study. The antenna with a merit of good production consistency exhibits an impedance bandwidth of 22% from 842 to 1049 MHz in the lower band, while the upper band covers 100 MHz (from 2.4 to 2.5 GHz). The measured peak gain is 3dBi and 5dBi at 915 MHz and 2.45 GHz, respectively.**

***Index Terms*—Dual-band, low-profile, gap-coupled feed, RFID, three-dimensional, silence element.**

I. Introduction

The Radio-frequency identification (RFID) technology has had a profound impact on human society in recent years. More and more enterprises and government utilize the RFID technology to collect and manage information. There is a fact that a lot of the frequency bands, such as 915 MHz (ISO 18000-6) and 2.45 GHz (ISO 18000-4) [1], are used in RFID applications. One antenna that meets different frequency bands not only saves space, but also improves the versatility of the system. Combined antenna, which usually consists of different radiators to realize different frequency bands, is one of the effective ways to achieve multi-band. Furthermore, silence element can reduce the interaction between these bands remarkably [2].

A number of research efforts have been devoted to the patch dual-band antenna [3]–[5], but a few studies pay attention to three-dimensional (3D) dual-band antenna. Three-dimensional omni-directional antenna is a common type of base station antennas, which have many advantages on the large-scale deployment of RFID applications. In [6], an eighth-wavelength 3D antenna composed of a conical monopole with metallic parasitic elements and a capacitive disk was proposed to achieve the characteristics of broadband and low-profile. Its drawback is too expensive to fabricate. A modified 3D RFID antenna [7] using printing technology is much cheaper. However, there are four tuning poles in that antenna. These tuning poles make it complex to manufacture and can be damaged easily.

In this study, a low-profile dual-band 3D antenna covering bands of 915 MHz and 2.45 GHz is presented. Two wedge patch tuning elements, contributing to the production consistency and reliability, are used to replace the four tuning poles in [7]. Independent quarter-wavelength patch radiators at 2.45 GHz, namely silence elements, are added to realize dual-band.

The paper is organized as follows. Section II gives the principle of the combined antenna with silence elements and describes the configuration of the proposed antenna in details. Section III offers the design process and simulation discussion. Results are presented in Section IV. The conclusions are outlined in Section V.

II. Antenna Principle And Configuration

Radiating structures in combined antenna are usually distinct, but the coupling caused by the adjacent radiators will change the single radiator's performance such as input impedance and radiation patterns. Antenna with silence elements can reduce these problems. Fig. 1 shows an ideal combined antenna with silence elements. Suppose $f1$ and $f2$ are the center frequencies in two bands. A_{f1} and A_{f2} are two separate antennas designed to work at $f1$ and $f2$, respectively. When the antenna operates at $f1$, all of the input energy should be fed into A_{f1}. On this occasion, A_{f1} is the active radiator in this band, while A_{f2} is the silence element, and vice versa. In fact, due to the inevitable presence of mutual coupling between radiators, the silence element also has a few negative impacts on the effective radiated body [2].

According to the concept of silence element, a new dual-band 3D antenna is proposed. The configuration of the antenna is shown in Fig. 2 (a). The antenna is fed by coplanar wave guide with ground, and a metal reflector ground plane is adopted to enhance the gain. There are three parts used for 915 MHz. Two identical printed triangular patchs perpendicularly connect to each other which can increase the current path and enhance the bandwidth. A disc loading on the top further reduces the height of the antenna. Wedge-shaped tuning patches are placed on the both sides of the triangular patch in order to improve production consistency and ameliorating the impedance matching. Two quarter-wavelength patches fed by gaps work at 2.45 GHz, shown in Fig. 2 (b). All the parts of the antenna are fabricated on FR4 substrate with a relative dielectric constant of 4.4 and thickness of 1.6mm.

III. Design And Simulation

The proposed antenna is designed to improve the production consistency and cover two bands required for RFID applications. In addition, mutual coupling between radiators is the key point in combined antenna design too. These issues are discussed below.

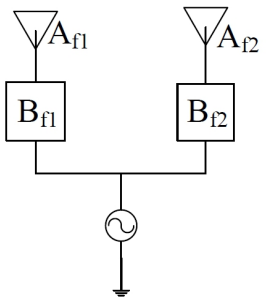

Fig. 1. Combined Antenna [2].

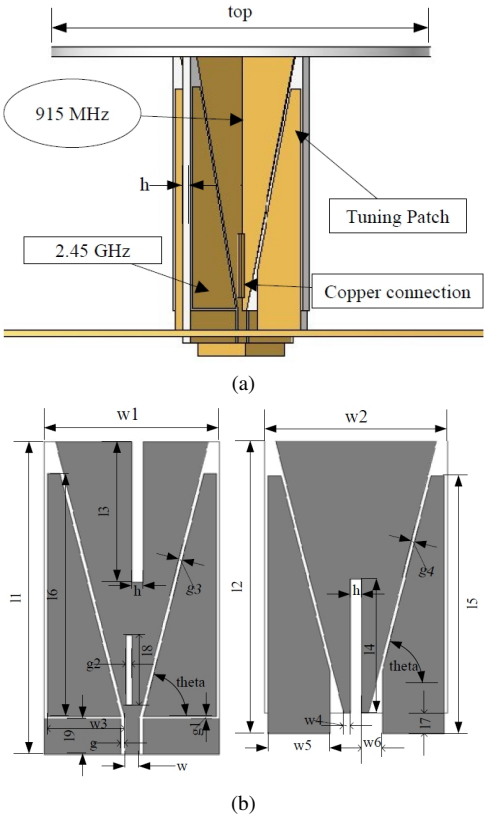

Fig. 2. Model of the antenna (a) whole (b) 2.45 GHz side on left and tuning side on right.

A. Patch Tuning Elements

Though the triangular monopole and the top loading disk can cut down the height of antenna, the input impedance of antenna in [7] still exhibits inductive characteristic without tuning poles. By introducing some capacitive elements, inductive reactance can be compensated. In this paper, two wedge tuning patches are adopted to improve the matching and promote the production consistency.

Two adjacent electrical conductors can constitute a capacitor. As a result of the small gap between triangular monopole and wedge patches, the capacitive reactance is significantly increasing. The equivalent circuit of matching network is given in Fig. 3 (a). The antenna, consisting of components R and L,

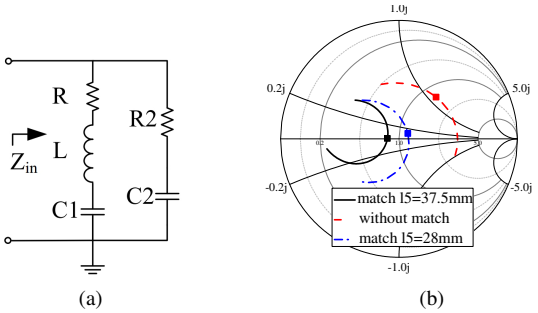

Fig. 3. Equivalent circuit and smith chart (a) equivalent circuit (b) input impedance with square marks at 915 MHz.

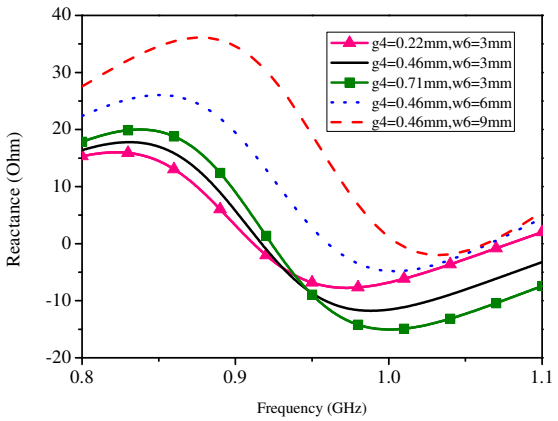

Fig. 4. Effect of $g4$ and $w6$ on reactance of input impedance.

will be modeled as a series resonator. By selecting the values of $C1$, $R2$ and $C2$, a complete cancellation of the reactive part of the input impedance at 915 MHz can be accomplished, as indicated in Fig. 3 (b). What's more, the impedance bandwidth is expanding too.

According to the principle of equivalence [8], width ($g4$) and length ($w6$) of the gap have an observable effect on the value of capacitor $C1$. The reactance is decreasing by reducing $g4$ and $w6$ that can be proved in Fig. 4. Owing to the gradual change structure, the matching patches have become a part of antenna and also affect the real part of input impedance. Here we introduce shunt-connected parasitic resistance $R2$ and parasitic capacitance $C2$. From simulation data in Fig. 3 (b), we can see the altitude of wedge patches is one of the factors for $R2$. The higher the altitude is, the smaller the real part of the input impedance is. The reasonable height is optimized for 37.5 mm.

B. Radiator at 2.45GHz

Two symmetric wedge-shaped quarter-wavelength patches are intended to add a frequency band of 2.45 GHz. The current on triangular patches is mainly distributed along the edges [7], so energy will feed into wedge-shaped patches through gaps. These two wedge-shaped patches are basically planar monopoles. So it's crucial that the length determines

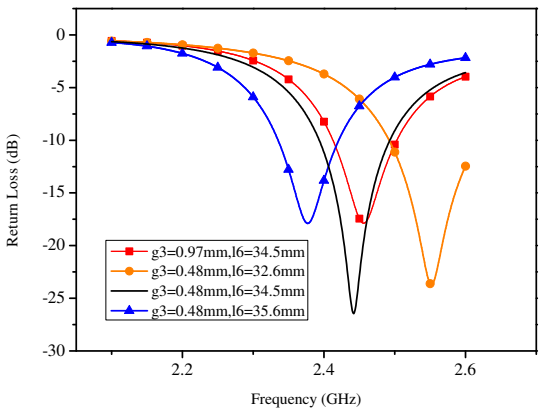

Fig. 5. Effect of $g3$ and $l6$ on return loss of antenna.

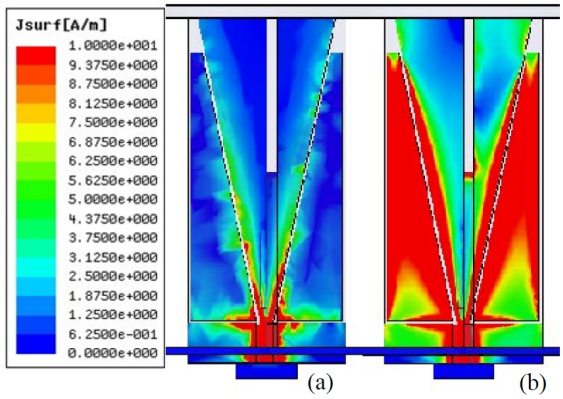

Fig. 6. Current distribution of antenna (a) 915 MHz (b) 2.45 GHz.

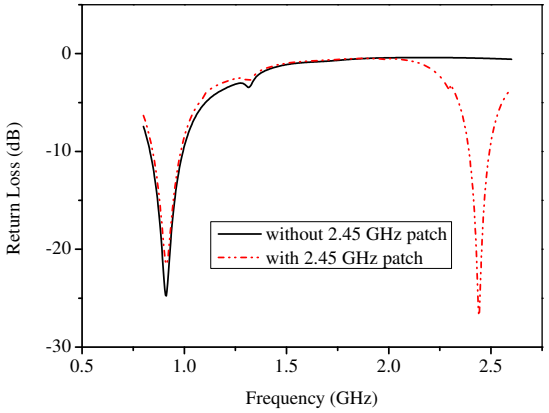

Fig. 7. Comparison of return loss.

the position of the resonance frequency. In Fig. 5, the centre frequency moves to a higher frequency when the length $l6$ is decreasing. The optimal dimensions will be $l6$=34.5mm at 2.45 GHz. The centre frequency moves to lower frequency when g3 is decreasing because the coupling gaps also have an influence on this band.

C. Mutual Coupling Between Radiators

The mutual coupling between radiators is an interesting problem in combined antenna. As in Fig. 1, if we take the 915 MHz radiator of the antenna as A_{f1}, then B_{f1} is considered in the straight-through state. On the other hand, A_{f2} is the wedge-shaped quarter-wavelength patches and B_{f2} is a complex coupling network. In most cases, the coupled A_{f2} will contribute to A_{f1} in the same frequency. But in this study, the appropriate gaps can hinder energy transferring to A_{f2} at 915 MHz approximately like a high-pass filter. Fig. 6 shows the current distribution of the antenna at 915 MHz and 2.45 GHz using HFSS. It is obvious that when the antenna is operating at 915 MHz, the current density of 2.45 GHz patches is extremely tiny. While in band of 2.45 GHz, the current density is quite large. So the 2.45 GHz patches mainly work in the higher frequency. After removing the 2.45 GHz patches, the return loss is investigated in Fig. 7. The result shows that the lower frequency band has little change and the higher frequency band totally disappears. It demonstrates that the 2.45 GHz patches are the silence elements and are transparent to the frequency band centered at 915 MHz.

IV. Measured Results

After the analysis and optimization, the design parameters are selected for the proposed antenna and they are reported in Table I. The photograph of the fabricated antenna is shown in Fig. 8. The overall height is $59mm \times 59mm \times 45mm$. The comparison between simulated and measured return loss is given in Fig. 9. The solid and the dashed lines denote the measured and simulated return loss, respectively. The antenna exhibits a measured -10 dB return loss bandwidth of 915 MHz,

TABLE I
Design Parameters of The Proposed Antenna (Unit: Millimeters)

w	$w1$	$w2$	$w3$	$w4$	$w5$	$w6$	top
2	24.9	26.5	11	1	9	3	59
$l1$	$l2$	$l3$	$l4$	$l5$	$l6$	$l7$	$l8$
44.5	42.5	20	19.5	37.5	34.5	3	10
$l9$	g	$g1$	$g2$	$g3$	$g4$	h	$theta$
5	0.6	0.4	0.8	0.48	0.46	1.6	76°

from 842 MHz to 1.049 GHz, and a high-frequency bandwidth of 2.45 GHz, from 2.4 GHz to 2.5 GHz. Fig. 10 and Fig. 11 show the measured and simulated H-plane and E-plane radiation patterns at 915 MHz and 2.45 GHz, respectively. Both of them are omni-directional in H-plane and tilt by around 30 degrees in E-plane due to the reflection of disk ground. The measured peak gain is 3 dBi at 915 MHz and 5 dBi at 2.45 GHz, as shown in Fig. 12.

V. Conclusion

In this work, a low-profile combined RFID antenna operating at 915 MHz and 2.45 GHz has been designed and fabricated.

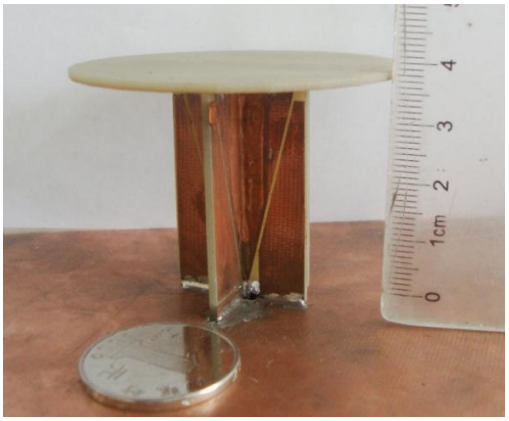

Fig. 8. Photograph of the fabricated antenna.

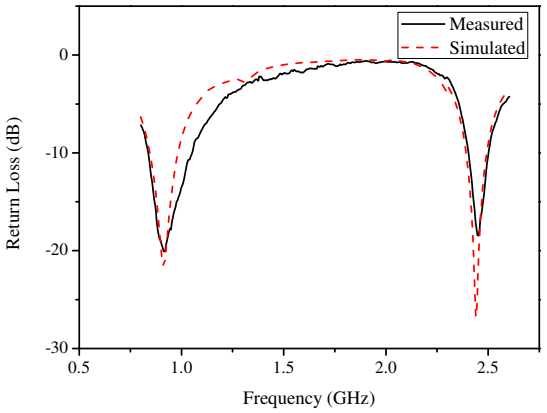

Fig. 9. Measured and simulated return loss of the proposed antenna.

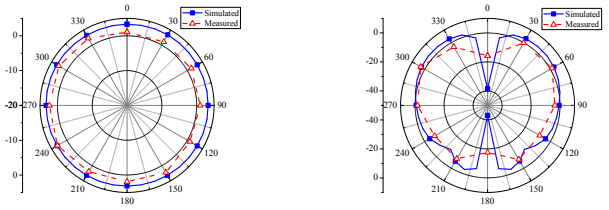

(a) (b)

Fig. 10. Radiation pattern at 915 MHz (a) H-plane (b) E-plane.

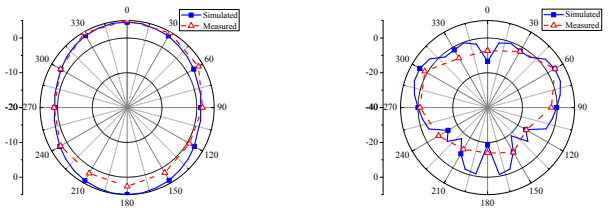

(a) (b)

Fig. 11. Radiation pattern at 2.45 GHz (a) H-plane (b) E-plane.

The overall antenna height is about eighth-wavelength at 915 MHz. The silence element is introduced to realize dual-band and it has little effect on the band of 915 MHz. Instead of conventional tuning poles, the wedge-shaped tuning patches make the antenna easy to design and fabricate. Radiation pattern in both bands is omni-directional and the gain is acceptable, which is very competitive for applications of wireless RFID systems.

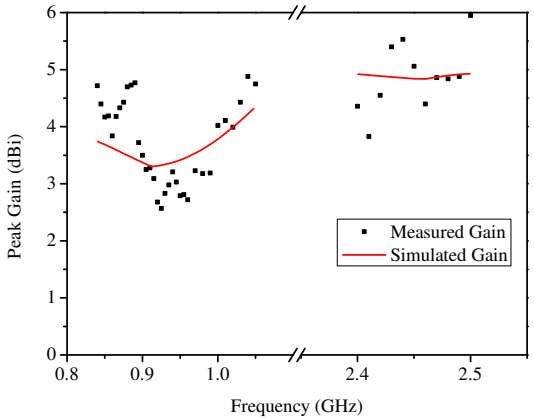

Fig. 12. Simulated and measured gain of the proposed antenna.

ACKNOWLEDGMENT

This work was supported in part by Suzhou Key Laboratory of RF and Microwave Millimeter Wave Technology, and in part by the Natural Science Foundation of the Higher Education Institutions of Jiangsu Province under Grant No. 12KJB510030. The authors would like to thank the staffs of the Jointed Radiation Test Center of Soochow University.

REFERENCES

[1] M. Grilo, F. Arnold, M. Gonçalves, L. Bravo-Roger, A. Moretti, and I. Lima, "Novel dual-band rfid antenna configuration with independent tuning adjustment," *Microwave and Optical Technology Letters*, vol. 54, no. 9, pp. 2214–2217, 2012.

[2] H. Guo, W. Cai, C. Zhou, and X. Liu, "Design and realization of a new combined multi-band antenna," *Chinese Journal of Radio Science*, vol. 2, p. 039, 2008.

[3] Z. L. Ma, L. J. Jiang, J. Xi, and T. Ye, "A single-layer compact hf-uhf dual-band rfid tag antenna," *Antennas and Wireless Propagation Letters, IEEE*, vol. 11, pp. 1257–1260, 2012.

[4] A. Mobashsher and R. Aldhaheri, "An improved uniplanar front-directional antenna for dual-band rfid readers," *Antennas and Wireless Propagation Letters, IEEE*, vol. 11, pp. 1438–1441, 2012.

[5] F. Paredes, G. Zamora, F. Herraiz-Martinez, F. Martin, and J. Bonache, "Dual-band uhf-rfid tags based on meander-line antennas loaded with spiral resonators," *Antennas and Wireless Propagation Letters, IEEE*, vol. 10, pp. 768–771, 2011.

[6] S. Palud, F. Colombel, M. Himdi, and C. Le Meins, "A novel broadband eighth-wave conical antenna," *Antennas and Propagation, IEEE Transactions on*, vol. 56, no. 7, pp. 2112–2116, 2008.

[7] L. Tian, H. Guo, X. Liu, Y. Wang, and X. Yang, "Novel 3d rfid antenna with low profile and low cost," in *Antennas, Propagation EM Theory (ISAPE), 2012 10th International Symposium on*, 2012, pp. 69–72.

[8] X. Liu and H. Guo, *Microwave technology and antennas (Chinese)*. Xidian University Press, 2007.